ON THE DESIGN OF AN ANTHROPOMORPHIC EYE SYSTEM USED IN THE NEW VERSION OF THE SOCIAL ROBOT PROBO

Florentina Adascalitei[1], Ioan Doroftei[1], Ovidiu Crivoi[1], Bram Vanderborght[2], Dirk Lefeber[2]

[1] *"Gh. Asachi" Technical University of Iasi, Romania, Mechanical Engineering, Mechatronics and Robotics Department, e-mail: adascalitei_florentina@yahoo.com, idorofte@mail.tuiasi.ro, crivoi2003@yahoo.com*

[2] *Vrije Universiteit Brussel (VUB), Belgium, e-mail: bram.vanderborght@vub.ac.be, dirk.lefeber@vub.ac.be*

Abstract: *The purpose of this study is to present the design of an anthropomorphic eye system which will be used in the new version of the social robot Probo. Due to the fact that the main goal is to achieve social children-robot interaction, the robot must have a number of social skills, like the capacity to imitate or to show emotions. Taking into account this requirements, a 10 degrees of freedom compact eye system was developed, which includes the eyeballs, the eyelids and the eyebrows. The eyes are necessary to create facial expressions, to enable eye-gaze based interaction or to be used as an active vision system, if they are equipped with small cameras. Because the eye-system design is based on a natural anthropomorphic model, the knowledge of anthropomorphic eyes anatomy and their movements it was a necessary requirement. Last, but not least, some mathematical models of the eye mechanisms used in the development process will be highlighted.*

Keywords: *design, eye system, modeling, Probo, social robot*

1. Introduction

In recent years there has been a growing interest in developing more intelligent interface between humans and robots, and improving all aspects of the interaction. For the robot to express a full range of emotions and to establish a face-to-face communication with a human being, nonverbal communications such as body language and facial expressions is vital. The ability to mimic human body and facial expressions lays the foundation for establishing a meaningful nonverbal communication between humans and robots [2]. [6] stated that body language and nonverbal communication represents 55% of the communication of feelings and attitudes. Through facial expressions, robots can display their own emotion just like human beings. The expressive behaviour of robotic faces is generally not life-like. For example, transitions between expressions tend to be abrupt, occurring suddenly and rapidly, which rarely occurs in nature. To render facial expressions the primary facial components used are mouth (lips), cheeks, eyes, eyebrows, neck and forehead.

To project humanness a robot must have eyes, and the eyes should include some complexity in surface detail, shape of the eye, eyeball, iris, and pupil. Hence, there are various reasons why a robot should be equipped with actuated eyes. First of all, the eyes are used to show facial expressions (none of the basic facial expressions can be realised by a robotic face without eyes). Furthermore, the eyes can be used to enable eye-gaze based interaction. When two people cross their gaze, they have eye contact. This enables communication [7]. A third reason is the fact that eyes can be used as an active vision system if they contain small cameras.

Another important aspect in the achievement of a natural anthropomorphic eye

system is related to the visibility of the mechanical parts. A solution to overcome this problem is by supporting the eye-ball spheres in an orbit [4].

So, in the development of a new version of the social robot Probo [4], one of the major challenges was to achieve the emotional behavior of the robotic face through facial expressions. Since the robot was meant to be used in child-robot interaction, a necessary requirement for the robot was to have the ability to show facial expressions. In order to perform various emotional expressions, the robot (Figure 1) was equipped with 21 degrees of freedom (d.o.f.), grouped in five subsystems, as follows: eye system (10 d.o.f.), ear system (2 d.o.f.), trunk system (3 d.o.f.), mouth system (3 d.o.f.) and neck system (3 d.o.f.). In the next paragraphs, our attention will be focused on the eye system, in terms of design, construction and modeling.

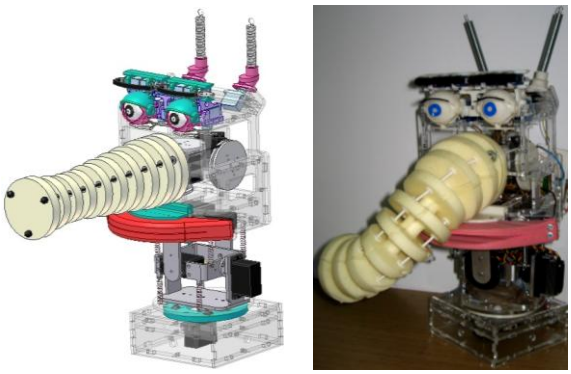

Figure 1: *New version of the robot Probo - CAD model and real prototype*

2. Anthropomorphic eye system

2.1 Mechanical design of the eye-system

Based on anatomical data, in many species, the eyes and its appendages are inset in the portion of the skull known as the orbits or eye sockets. The movements of different body parts are controlled by striated muscles acting around joints. The movements of the eye are no exception [5]. Each eye has six extra-ocular muscles that control its movements: the lateral rectus, the medial rectus, the inferior rectus, the superior rectus, the inferior oblique and the superior oblique.

When the muscles exert different tensions, a torque is exerted on the globe causing it to turn. This is an almost pure rotation, with only about one millimeter of translation [4]. As it is a globe inside a socket three motions can be considered, abduction/adduction, elevation/ depression and rotation. The muscles have combined actions to achieve these motions, but each eye is completely independent of the other.

Because the eye-system design is based on a natural anthropomorphic model it gives the impression of being natural. Eye-gaze based interaction is a powerful social cue that people use to determine what interests others. By directing the robot's gaze to the visual target, the person interacting with the robot can accurately use the robot's gaze as an indicator of what the robot is attending to. This greatly facilitates the interpretation and readability of the robot’s behavior, since the robot reacts specifically to what it is looking at [1].

The eye system (Figure 2) includes the eyeballs (4 d.o.f.), the eyelids (2 d.o.f.) and the eyebrows (4 d.o.f.).

Compared with the previous version, this new solution has an additional degree of freedom providing independent motions for all the actuated parts. Eyeballs are designed to enhance the interaction with people based on human anthropomorphic data. The eyes can pan and tilt independently, the eyelids can enable the eyes to open and close at various degrees and the motion of eyebrows intensifies the facial expressions. The movement ranges of the eye system are presented in Table 1.

Table 1: *Eye movements and ranges*

Movement	Range [°]
Left, Right Eye Pan	±45
Left, Right Eye Tilt	±45
Left, Right Eyelid	70
Left, Right Eyebrow Left	±10
Left, Right Eyebrow Right	±10

The conceptual idea was to hold the eyes in an orbit as discussed in the previous paragraph. In our case, the eyeballs (35 mm) are placed in two eye-supports, assuring the necessary space for a spherical motion of the

eyeballs. All the components are made from ABS plastic, due to its good mechanical properties (impact resistance, toughness), using rapid prototyping extrusion-based 3D printers.

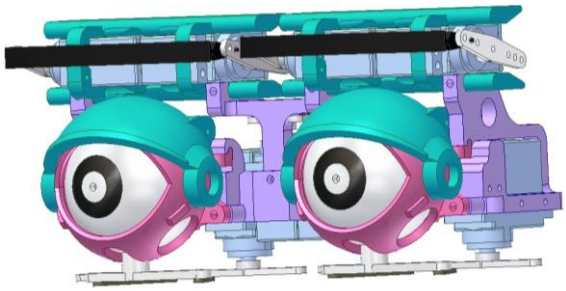

(a)

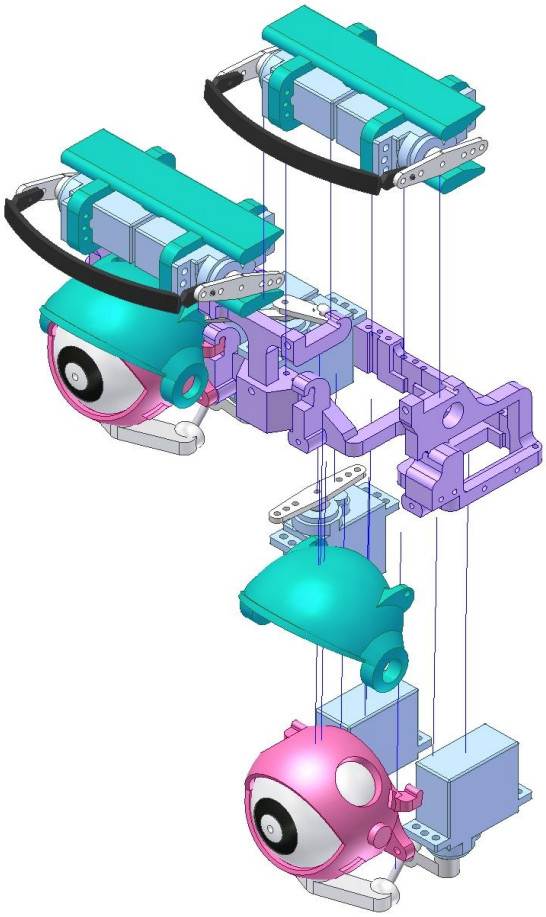

(b)

Figure 2: *Design of the eye-system: a) compact view; b) exploded view of one eye*

When a robot is intended to interact with people, it requires an active vision system that can fulfill both a perceptual and a communicative function. For that reason, the designed eyes are hollow and can contain small cameras. As its cameras can move, the range of the visual scene is not restricted to that of the static view. But, in a preliminary phase, the robot will be equipped with only one camera, placed between the eyebrows. The reason is to maintain operational the active vision system even when the robot is sleeping and its eyes are closed.

The eyebrows are made from an elastic material, that allows their deformation when only a single servo is actuated, or both, but in opposite ways.

In the previous design, eyes were operated through flexible Bowden cables and the motors were mounted in the belly of the robot. Under the new concept the components are driven directly (eyebrows) or through bar mechanisms, with spherical joints (eyeballs and eyelids), mounted on the shaft coupling. The entire eye system is actuated with 10 digital hobbyist servo motors HS 5055MG.

The motion of the eyes is provided with the use of four bar mechanisms, with spherical joints. Each eye is actuated with two servos. So, if only a single servo is actuated, we obtain the motion called eye tilt (the eye is moving to the left or to the right); if both servos are working, but in opposite ways, we get eye pan (up-down).

2.2 Kinematics

2.2.1 Eyelid module

We will first consider the eyelid subsystem. The design of an eyelid is shown in Figure 3.a and its kinematics in Figure 3.b. A RSUR spatial linkage is used to connect the servo axes to the rotational joint of the eyelid.

In order to solve direct kinematics, an equivalent mechanism is used (see Figure 4). First, if we apply standard Denavit - Hartenberg convention to this closed-loop mechanism, we get the parameters presented in Table 2. Based on these, we will write the transition homogeneous transformation matrixes that express the position and orientation of the current frame with respect to the previous one. Multiplying all these matrixes we will get the total homogeneous

transformation matrix of the mechanism that expresses the position and orientation of the last frame with respect to the referential frame.

The orientation loop closure equation for our mechanism can be written as following

$$ {}^{0}_{4}R = {}^{0}_{1}R \cdot {}^{1}_{2}R \cdot {}^{2}_{2'}R \cdot {}^{2'}_{2''}R \cdot {}^{2''}_{3}R \cdot \cdot {}^{3}_{3'}R \cdot {}^{3'}_{4}R = I \qquad (1) $$

where ${}^{i-1}_{i}R$ is the transition orientation matrix that express the orientation of the $\{i\}$ frame with respect to the $\{i-1\}$ frame.

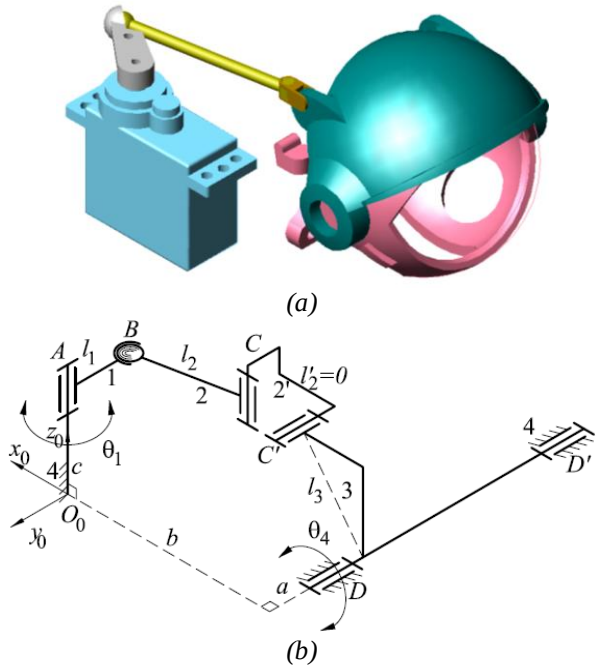

Figure 3: *Eyelid subsystem: a) design; b) kinematics*

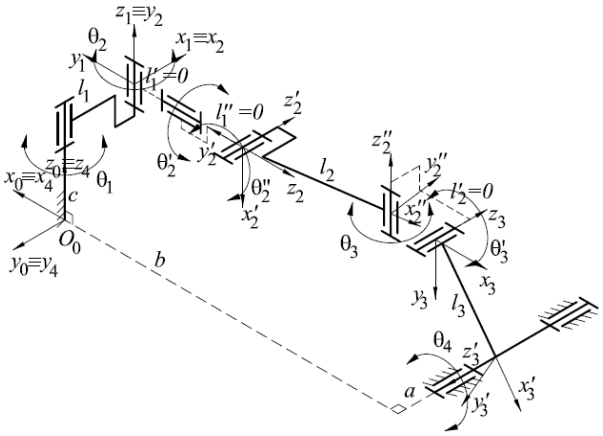

Figure 4: *Equivalent eyelid mechanism kinematics*

Table 2: *Standard Denavit_Hartenberg parameters*

Link	a_i	α_i	d_i	θ_i
1	l_1	0	c	θ_1
2	0	$\pi/2$	0	θ_2
2′	0	$-\pi/2$	0	θ_2'
2″	l_2	$\pi/2$	0	θ_2''
3	0	$-\pi/2$	0	θ_3
3′	l_3	$-\pi/2$	0	θ_3'
4	b	$-\pi/2$	a	θ_4

The position loop closure equation can be written as following

$$ \bar{r}_1 + \bar{r}_2 + \bar{r}_3 + ... + \bar{r}_n = \bar{0} \qquad (2) $$

where $\bar{r}_i$ is a vector drawn from the origin of the frame $\{i-1\}$ to the origin of the $\{i\}$ frame.

The following equation is obtained according to standard Denavit - Hartenberg convention,

$$ {}^{0}\bar{r}_i = d_i \cdot {}^{0}_{i-1}R \cdot \bar{z} + a_i \cdot {}^{0}_{i}R \cdot \bar{x} \qquad (3) $$

where ${}^{0}\bar{r}_i$ represents the column matrix form of $\bar{r}_i$ defined in $\{0\}$ referential.

Thus equation (2) can be written in the following form,

$$ d_1 \cdot \bar{z} + a_1 \cdot {}^{0}_{1}R \cdot \bar{x} + d_2 \cdot {}^{0}_{1}R \cdot \bar{z} + a_2 \cdot {}^{0}_{2}R \cdot \bar{x} + \\ + ... + d_n \cdot {}^{0}_{n-1}R \cdot \bar{z} + a_n \cdot {}^{0}_{n}R \cdot \bar{x} = \bar{0} \qquad (4) $$

The loop closure equations written above are two fundamental matrix equations by which the general displacement equation of any spatial linkage is obtained. According to equation (4), the next equation can be written for our mechanism

$$ c \cdot \bar{z} + l_1 \cdot {}^{0}_{1}R \cdot \bar{x} + l_2 \cdot {}^{0}_{2''}R \cdot \bar{x} + l_3 \cdot {}^{0}_{3'}R \cdot \bar{x} + \\ + a \cdot {}^{0}_{3'}R \cdot \bar{z} + b \cdot {}^{0}_{4}R \cdot \bar{x} = \bar{0} \qquad (5) $$

Considering equation (1), next equations are obtained,

$$ {}^{0}_{2''}R = {}^{2''}_{4}R^{-1} = \left({}^{2''}_{3}R \cdot {}^{3}_{3'}R \cdot {}^{3'}_{4}R \right)^{-1} = $$

$$ = \begin{bmatrix} c_3c_{3'}c_4 + & s_3c_{3'}c_4 - & -s_{3'}c_4 \\ +s_3s_4 & -c_3s_4 & \\ c_3s_{3'} & s_3s_{3'} & c_{3'} \\ -c_3c_{3'}s_4 + & -s_3c_{3'}s_4 - & s_{3'}s_4 \\ +s_3c_4 & -c_3c_4 & \end{bmatrix} \qquad (6) $$

$$ {}^{0}_{3'}R = {}^{3'}_{4}R^{-1} = \left(R_z(\theta_4) \cdot R_x(-\pi/2) \right)^{-1} = $$

$$ = \begin{bmatrix} c_4 & s_4 & 0 \\ 0 & 0 & -1 \\ s_4 & c_4 & 0 \end{bmatrix} \qquad (7) $$

$$ {}^{0}_{4}R = I = \begin{bmatrix} 1 & 0 & 0 \\ 0 & 1 & 0 \\ 0 & 0 & 1 \end{bmatrix} \qquad (8) $$

where $s_i = \sin\theta_i$, $c_i = \cos\theta_i$, for $i = 0 \ldots 4$.

Substituting from (6)-(8) into equation (5), we get

$$ \begin{gathered} c \cdot \bar{z} + l_1 \cdot c_1 \cdot \bar{x} + l_1 \cdot s_1 \cdot \bar{y} + \\ + l_2 \cdot \left(c_3c_{3'}c_4 + s_3s_4 \right) \cdot \bar{x} + \\ + l_2 \cdot c_3s_{3'} \cdot \bar{y} + l_2 \cdot \left(-c_3c_{3'}s_4 + s_3c_4 \right) \cdot \bar{z} + \\ + l_3 \cdot c_4 \cdot \bar{x} - l_3 \cdot s_4 \cdot \bar{z} - a \cdot \bar{y} + b \cdot \bar{x} = \bar{0} \end{gathered} \qquad (9) $$

which results in the following equations,

$$ \begin{cases} l_1 \cdot c_1 + l_2 \cdot \left(c_3c_{3'}c_4 + s_3s_4 \right) + l_3 \cdot c_4 + b = 0 \\ l_1 \cdot s_1 + l_2 \cdot c_3s_{3'} - a = 0 \\ c + l_2 \cdot \left(-c_3c_{3'}s_4 + s_3c_4 \right) - l_3 \cdot s_4 = 0 \end{cases} \qquad (10) $$

If we multiply the three equations by themselves and we add the results, we get

$$ \begin{gathered} 2 \cdot l_3 \cdot \left(l_1 \cdot c_1 - b \right) \cdot c_4 + 2 \cdot c \cdot l_3 \cdot s_4 = \\ = l_1^2 - l_2^2 + l_3^2 + a^2 + b^2 + c^2 - 2 \cdot a \cdot l_1 \cdot s_1 - \\ - 2 \cdot b \cdot l_1 \cdot c_1 \end{gathered} \qquad (11) $$

Equation (11) is called the general displacement equation of the *RSUR* linkage and plays a key role in mobility analysis and function generation synthesis of the mechanism.

Let $p(\theta_1) = 2 \cdot l_3 \cdot (l_1 \cdot c_1 - b)$, $q = 2 \cdot c \cdot l_3$, $r(\theta_1) = l_1^2 - l_2^2 + l_3^2 + a^2 + b^2 + c^2 - 2 \cdot a \cdot l_1 \cdot s_1 - -2 \cdot b \cdot l_1 \cdot c_1$.

Thus equation (11) is written in the following form,

$$ p(\theta_1) \cdot \cos\theta_4 + q \cdot \sin\theta_4 = r(\theta_1) \qquad (12) $$

Now, let $\cos\theta_4 = \frac{1 - t^2}{1 + t^2}$ and $\sin\theta_4 = \frac{2t}{1 + t^2}$. Hence equation (12) becomes

$$ \begin{gathered} \left(r(\theta_1) + p(\theta_1) \right) \cdot t^2 - 2qt + \\ + r(\theta_1) - p(\theta_1) = 0 \end{gathered} \qquad (13) $$

which results in,

$$ t = \frac{q \pm \sqrt{p^2(\theta_1) + q^2 - r^2(\theta_1)}}{p(\theta_1) + r(\theta_1)} \qquad (14) $$

Thus next equation is derived

$$ \theta_4 = A\tan 2\left(\frac{2t}{1 + t^2}, \frac{1 - t^2}{1 + t^2} \right) \qquad (15) $$

In order to prove the effectiveness of the spatial four-bar mechanism used to actuate the eyelid, a numerical simulation has been done. The real dimensional parameters (used in for the prototype) of this mechanism have been used for this simulation: $l_1 = 13$ [mm], $l_2 = 36$ [mm], $l_3 = 18$ [mm], $a = 14$ [mm], $b = 37$ [mm], $c = 13.4$ [mm].

The results of this simulation are shown in next figures: Figure 5 – diagrams, $\theta_1(t)$, $\theta_4(t)$; Figure 6 - the diagram $\theta_4(\theta_1)$; Figure 7 - diagrams of the angular velocities, $\omega_1(t)$, $\omega_4(t)$.

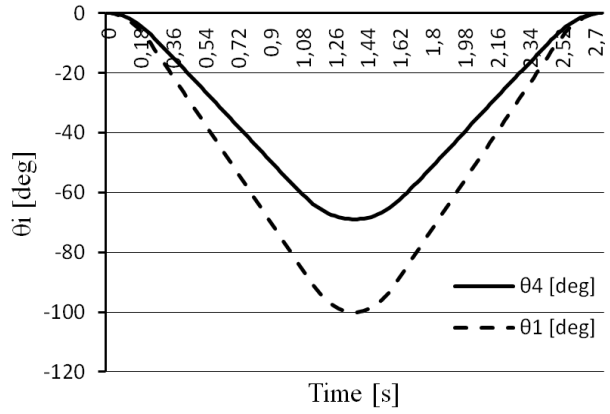

Figure 5: *Diagrams* $\theta_1(t)$, $\theta_4(t)$

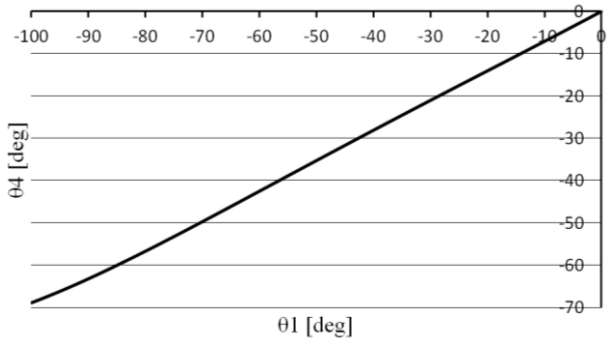

Figure 6: *Diagram* $\theta_4(\theta_1)$

As we see in Figure 6, the variation of the eyelid orientation angle, θ_4, according to the servo orientation angle, θ_1, is approximately linear, proving the effectiveness of the four-bar linkage. This fact has positive effect for orientation control of the eyelid, simplifying the algorithm.

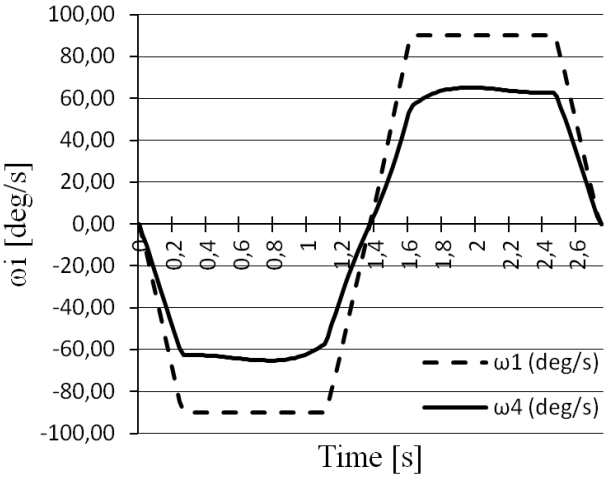

Figure 7: *Diagrams* $\omega_1(t)$, $\omega_4(t)$

2.2.2 Eyeball module

The eyeball subsystem has a more complex design because the eyeball itself should have a spatial motion (three rotations around all the axes of a Cartesian frame, it means 3 d.o.f.). Consequently, two servos and two spatial four-bar mechanisms in series are using to drive the eyeball.

A 3D view of the eyeball design is shown in Figure 8.a and its kinematics in Figure 8.b. Two *RSUR* spatial linkages in series (*ABCD* and *A'B'C'D*) and a supplementary link (and joint) are used to drive the eyeball. When the joints *A* and *A'* have equal angular velocities, the eyeball is rotating around its vertical axis. If these joints have equal and opposite angular velocities, the eyeball is rotating around its horizontal axis. Rotating these joints with different angular velocities, the eyeball will be rotated around a specific axis.

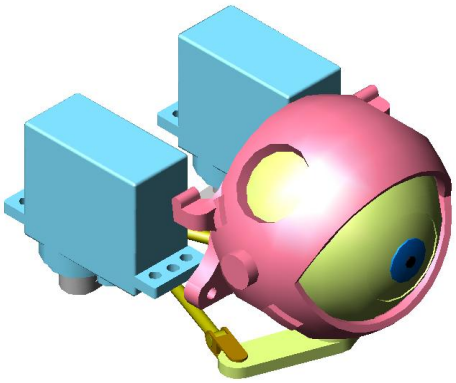

(a)

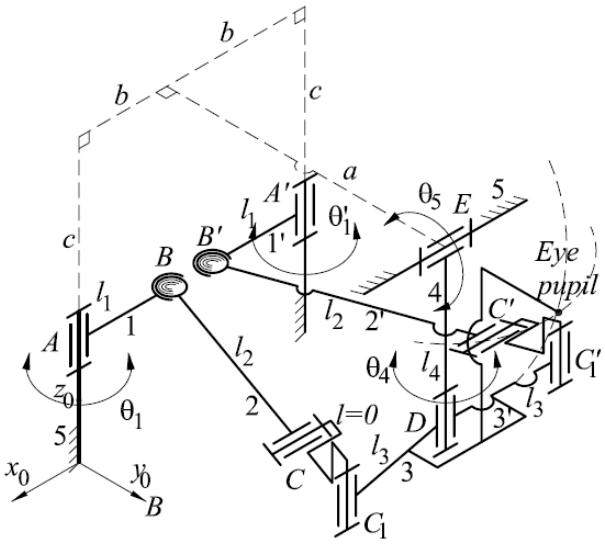

(b)

Figure 8: *Eyeball subsystem: a) design; b) kinematics*

Due to lack of space, in this paper only some simulation results of this mechanism will be presented. In our simulation, next parameters have been used: $l_1 = 13.5$ [mm], $l_2 = 35$ [mm], $l_3 = 16$ [mm], $l_4 = 22$ [mm], $a = 37$ [mm], $b = 16.5$ [mm], $c = 22$ [mm].

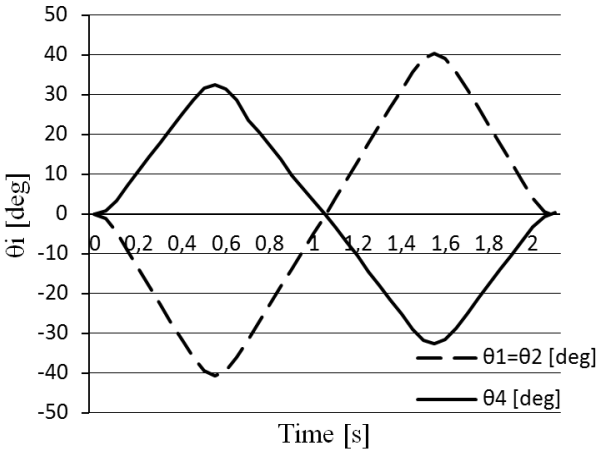

Figure 9: *Diagrams* $\theta_1(t)$, $\theta_2(t)$, $\theta_4(t)$, *the eyeball is moving right and left*

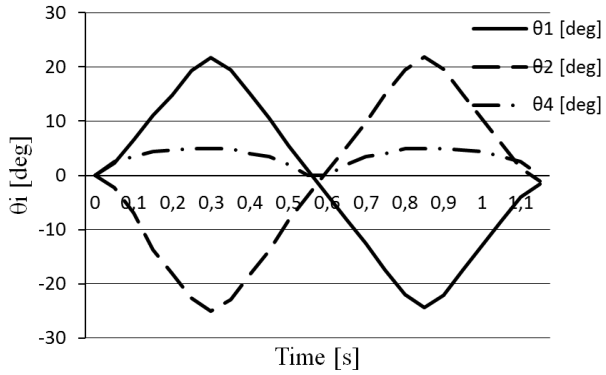

Figure 10: *Diagrams* $\theta_1(t)$, $\theta_2(t)$, $\theta_4(t)$, *the eyeball is moving up and down*

If we compare Figure 9 and Figure 10, we may conclude that, for the same rotation angle of the driven motor shafts (the same values of $\theta_1(t)$ and $\theta_2(t)$) the rotation angle of the driven link - the eyeball (the value of $\theta_4(t)$) for up and down movement is much smaller than the one corresponding to its horizontal movement.

2.2.3 Eyebrow module

The last subsystem of the eye system is the eyebrow, actuated by two servos (Figure 11).

When the links *1* and *5* are rotating in counterclockwise direction (the servos are actuated in opposite direction), the eyebrow is moving up otherwise it is moving down. If these links are rotating in opposite direction, the eyebrow will rotate around *y* axis.

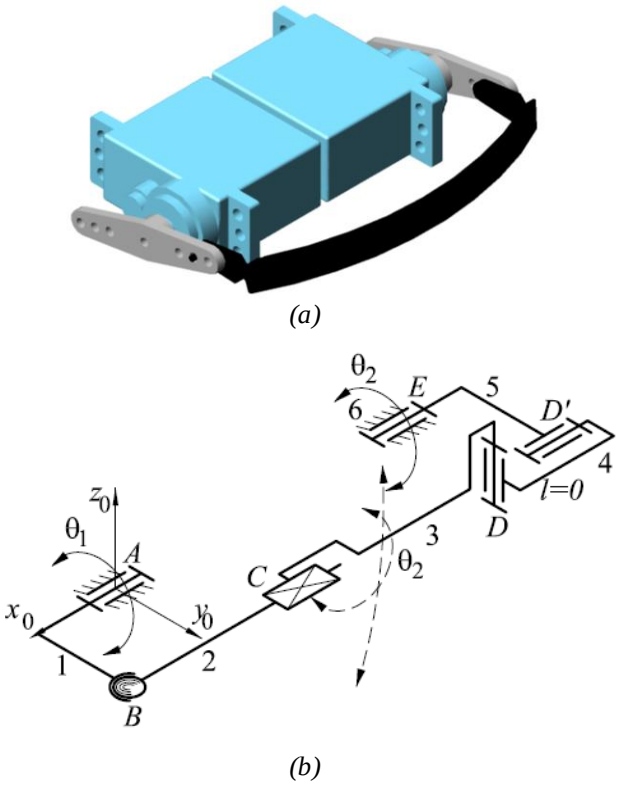

Figure 11: *Eyebrow subsystem: a) design; b) kinematics*

2.3 Experimental test

Till now, preliminary experimental tests have been done, to prove the effectiveness of all the robot head subsystems. For the eye subsystems, some pictures taken during these tests will be shown in Figure 12.

Summary

In this paper, a new conceptual design for an anthropomorphic eye system which is used in the development of the new version of the social robot Probo has been presented. Some kinematics aspects of the mechanism used to drive each subsystem of the eye system and, also, numerical simulations have been demonstrated. The subject will be more developed in another future paper.

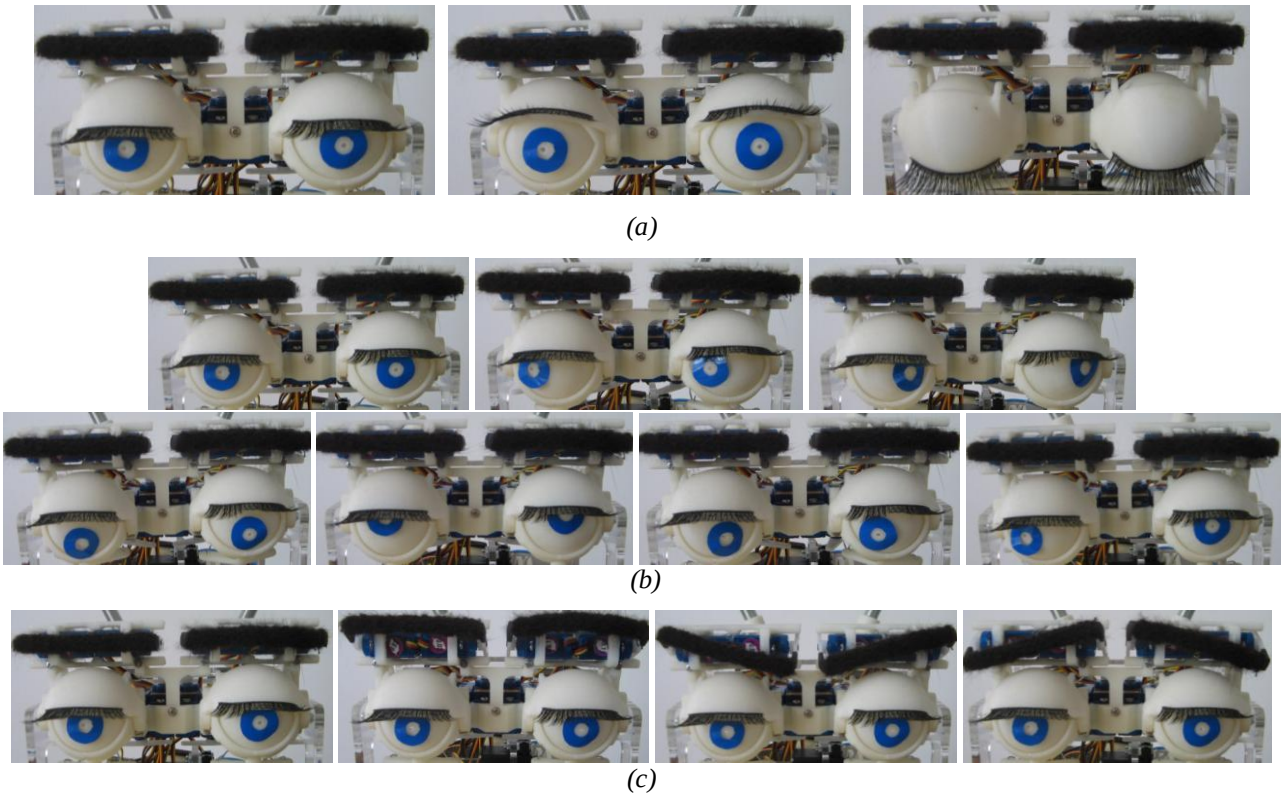

(a)

(b)

(c)

Figure 12: *Eye subsystem during tests: a) different positions of the eyelid; b) eyeball in different positions; c) possible positions of the eyebrow*

Acknowledgement

This paper was realized with the support of POSDRU CUANTUMDOC "Doctoral studies for European performances in research and innovation" ID79407 project, funded by the European Social Fund and Romanian Government. We are also grateful to the Robotics and MultiBody Mechanics Research Group (VUB) for their support and collaboration.

References

[1] Breazeal, C., *Regulation and Entrainment for Human-Robot Interaction*, D. Rus and S. Singh (Eds.), in: Int. Journal of Experimental Robotics, 21(10-11), pp. 883-902, 2002.

[2] Brethes, L., Lerasle, F., Danes, P, *Data fusion for visual tracking dedicated to human-robot interaction*, In Proceedings of the 2005 IEEE International Conference on Robotics and Automation, (Barcelona, Spain), pp. 2075-2080, 2005.

[3] Carpenter, R.H.S., *Movements of the Eyes (2nd ed.)*, Pion Ltd, London. ISBN 0850861098, 1988.

[4] Goris, K., Saldien, J., Vanderborght, B., Lefeber, D., *Mechanical design of the huggable robot Probo*, International Journal of Humanoid Robotics, Volume 8, Issue 3, pp.481-511, 2011.

[5] Goris, K., Saldien, J., Vanderborght, B., Verrelst, B., Van Ham, R., Lefeber, D., *The Development of the Eye-System for the Intelligent Huggable Robot ANTY*, CLAWAR, 2006.

[6] Mehrabian, A., *Silent Messages. Belmont*, CA: Wadsworth, ISBN 0-534-00910-7, 1971.

[7] Miyauchi, D., Sakurai, A., Nakamura, A., Kuno, Y., *Human-Robot Eye Contact through Observations and Actions*," IEEE, Int. Conference on Pattern Recognition, 2004.